

Diffusion in a rough potential revisited

Saikat Banerjee,¹ Rajib Biswas,¹ Kazuhiko Seki,² and Biman Bagchi^{1,*}

¹*Solid State and Structural Chemistry Unit, Indian Institute of Science, Bangalore - 560012, India*

²*National Institute of Advanced Industrial Science and Technology (AIST),
AIST Tsukuba Central 5 Higashi 1-1-1, Tsukuba, Ibaraki 305-8565, Japan*

Rugged energy landscapes find wide applications in diverse fields ranging from astrophysics to protein folding. We study the dependence of diffusion coefficient (D) of a Brownian particle on the distribution width (ε) of randomness in a Gaussian random landscape by simulations and theoretical analysis. We first show that the elegant expression of Zwanzig [PNAS, **85**, 2029 (1988)] for $D(\varepsilon)$ can be reproduced exactly by using the Rosenfeld diffusion-entropy scaling relation. Our simulations show that Zwanzig's expression overestimates D in an uncorrelated Gaussian random lattice – differing by almost an order of magnitude at moderately high ruggedness. The disparity originates from the presence of “three-site traps” (TST) on the landscape – which are formed by the presence of deep minima flanked by high barriers on either side. Using mean first passage time formalism, we derive a general expression for the effective diffusion coefficient in the presence of TST, that quantitatively reproduces the simulation results and which reduces to Zwanzig's form only in the limit of infinite spatial correlation. We construct a continuous Gaussian field with inherent correlation to establish the effect of spatial correlation on random walk. The presence of TSTs at large ruggedness ($\varepsilon \gg k_B T$) give rise to an apparent breakdown of ergodicity of the type often encountered in glassy liquids.

I. INTRODUCTION

The diffusion of a Brownian particle on a random energy landscape serves as an effective model in understanding different complex phenomena and can be considered as a historically important [1–6] problem. Examples include diffusion in glassy matrices and supercooled liquids [7–9], dynamics of molecular motors moving along heterogeneous substrates [10], diffusion of a protein along a DNA in search for a specific binding site [11], dynamics of fluorescently labeled molecules inside the cell [12, 13]. A highly topical application of this model is in protein folding where the transformation of the unfolded state is viewed as diffusion in polymer conformation space that contains multiple maxima and minima [14–17]. Yet another example is provided by enzyme kinetics where a broad distribution of relaxation times observed in single molecule spectroscopy has been attributed to random energy landscape experienced by the enzyme near the global minimum that determines its equilibrium configuration [18, 19]. For many years different variant of random energy barrier models have been used to study electron transport in disordered solids [20].

Despite the broad applicability and historical importance of the problem, there are surprisingly few numerical and simulation studies of this problem. As a result, we have little knowledge about the effect of ruggedness on diffusion at a quantitative level. Every study seems to use the expression of Zwanzig (discussed below) but the validity of the same has never been tested, although Zwanzig himself termed his derivation as “conjectural”. There have been studies on random traps and random

barriers, but true definition of ruggedness requires simultaneous presence of both. Diffusion in rugged landscape is thus quantitatively different from either random traps or random barriers.

Another important issue not touched upon adequately is the role of spatial correlations in the diffusion process. Ruggedness is expected to be correlated in many cases, such as protein diffusion along a DNA. Such correlations can alter the motion of a particle. Wolynes and co-workers have shown that the dynamics changes considerably in presence of correlations in protein folding funnels [21, 22] and glass transitions [23].

The dynamics of a free Brownian particle at time scales where inertia can be neglected is well understood since Einstein's seminal paper, and has been generalized in many different directions [24]. However, in the presence of a random potential with multiple maxima and minima, diffusion can become significantly different as the simultaneous presence of barriers and troughs can significantly and non-trivially retard the mean square displacement. Several models have been developed to understand the complex dynamics, *e.g.* the random trap model [25], the random barrier model [26, 27], continuous time random walk [8], etc. Theoretical analyses are mostly restricted to asymptotic long-time limits, when the particle motion should become diffusive. In an important treatment of the problem, Zwanzig [5] considered a general rough potential $U(x)$ with a smooth background $U_0(x)$ on which a perturbation $U_1(x)$ is superimposed, so that $U(x) = U_0(x) + U_1(x)$. He showed that the effective diffusion coefficient (D_{eff}) on the rough potential can be expressed as

$$D_{\text{eff}} = \frac{D_0}{\langle e^{\beta U_1} \rangle \langle e^{-\beta U_1} \rangle} \quad (1)$$

where D_0 is the bare diffusion coefficient on the smooth

* bbagchi@sscu.iisc.ernet.in

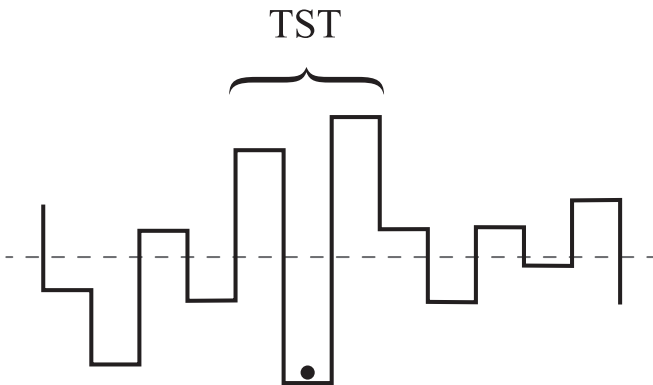


Figure 1. Schematic representation of “Three-Site Trap” (TST) on a lattice (not to scale). Unlike isolated extremely deep minimum or maximum, TST is formed when a deep minimum is flanked by high maxima on both sides. The probability of encountering a TST would be the joint probability of occurrence of such three sites simultaneously. Hence TSTs are more common than extremely sharp minima / maxima in a Gaussian random surface.

potential, $\beta = 1/k_B T$ and $\langle \dots \rangle$ denotes the spatial, *local* average used to smooth the perturbation. For a random potential, where the amplitude of roughness has a Gaussian distribution,

$$P(U_1) = \frac{1}{\varepsilon\sqrt{2\pi}} \left[\exp\left(-\frac{U_1^2}{2\varepsilon^2}\right) \right] \quad (2)$$

in which ε is the root-mean-squared roughness, $\varepsilon^2 = \langle U_1^2 \rangle$, Zwanzig showed that the effective diffusion coefficient $D_{\text{eff},z}$ can be given by the following simple and elegant expression,

$$D_{\text{eff},z} = D_0 \exp(-\beta^2 \varepsilon^2) \quad (3)$$

Note that we use the subscript on $D_{\text{eff},z}$ to refer Zwanzig’s work, and will use different subscripts as we discuss further for the sake of comparison and analyses. Despite the novelty of the work and simplicity of the expression, the derivation of the above invokes the questionable local averaging of the random energy surface (in the simplification of the double integral that arises while evaluating the MFPT). *Zwanzig himself was aware of the possible limitation of his approximate approach, and termed his final result as “conjectural”.*

There are multiple unanswered issues in this problem. First and foremost, the existence of diffusion itself could be doubtful at large ruggedness. Imagine that the particle encounters a situation where it is stuck in a deep minimum (negative energy) with maxima (barriers, positive energy) on its two sides. We refer to this as “three-site trap (TST)” (see Fig. 1). Such TSTs become increasingly probable as ruggedness (that is, ε) increases, and can give rise to long trapping and hence sub-diffusive growth of MFPT. In fact, such TSTs are ignored in the coarse-graining mentioned earlier. We find that exact evaluation of the MFPT deviates from and improves upon the

coarse-grained expression. Second, the MFPT approach to estimate the diffusion constant (comparing τ_{MFPT} with that of an effective flat potential, thereby implicitly invoking the relation $D_{\text{eff}} = L^2/2\tau_{\text{MFPT}}$ where τ_{MFPT} is the MFPT between an initial and final position separated by a distance L) might not work. Third, and a related issue, is the question of stationarity and ergodicity. Diffusion can be defined for a random process which is both stationary and ergodic. Even if we consider a random landscape which is stationary, the long trapping in the deep minima results in a “broken ergodicity” on such random potential energy surface, which has strong resemblance with the glass transition scenario. Modeling motion on such landscapes using standard methods of Monte Carlo is unreliable, and requires special asymptotic techniques [28, 29]. This paradigm for trapping on long timescales by metastable states in complex systems may be visualized as a terrain with lakes in the valleys whose water level depends on the observational timescale [30]. This is where the relationship between diffusion and entropy can have a role to play. Last but not the least, there could be a spatial correlation among the values of energy of the neighboring sites. Such a correlation adds a new dimension to the problem. Fortunately, we have been able to address all the four issues in this work.

II. ROSENFELD ENTROPY SCALING ON RUGGED ENERGY LANDSCAPE

The successful entropy-diffusion scaling relationship was first proposed by Rosenfeld in 1977 on the basis of extensive simulation results for the transport coefficients of a wide variety of one-component systems including those containing hard spheres, soft spheres, or plasma [31, 32]. Using macroscopic reduction parameters for the length as $\rho^{-1/3}$ and the thermal velocity as $(k_B T/m)^{1/2}$, Rosenfeld demonstrated that, in dimensionless units, the self-diffusivity D_0 of a bulk fluid is well correlated with the excess entropy in terms of an exponential relation

$$D_{\text{eff},R} = D_0 \frac{\rho^{1/3}}{(k_B T/m)^{1/2}} \approx a \exp(b S_{\text{ex}}) \quad (4)$$

where $S_{\text{ex}} = (S - S_{\text{id}})/Nk_B$ is the reduced excess (dimensionless) entropy per molecule, a and b are the constants which depend on the system, but b shows weak variation. Although Rosenfeld scaling relation is routinely used in varied contexts for understanding the relationship between thermodynamics, transport properties and potential energy landscape [33, 34], the validity of the relation was established by essentially empirical means. Another well-known relationship between entropy and diffusion in glassy liquids was given by Adam and Gibbs [35], and is of the following form,

$$D_{\text{eff},AG} = a \exp\left(-\frac{b}{T S_{\text{conf}}}\right) \quad (5)$$

where S_{conf} is the configurational entropy. In the intermediate temperature regime, both Rosenfeld and Adam-Gibbs seem to provide reliable descriptions, although at still lower temperature, in viscous liquid, Rosenfeld scaling becomes unreliable. Surprisingly, relationship between these two entropy-based relations has not been sufficiently explored.

A random energy landscape with Gaussian distribution allows an exact derivation of partition function, which leads us to the excess entropy. The connection between entropy and random energy landscapes was earlier discussed by Wolynes [36]. Such correlation helps us to connect the Rosenfeld scaling relation with Zwanzig's diffusion coefficient. Therefore, it provides an indirect way to theoretically validate the Rosenfeld scaling relation. Starting with the partition function (Q) for the random energy surface, we obtain free energy (A) and entropy (S) as,

$$Q = \sum_i \exp\left(-\frac{U_{1i}}{k_B T}\right) = N \exp\left(-\frac{\varepsilon^2}{2(k_B T)^2}\right) \quad (6)$$

$$A = -k_B T \ln Q = -k_B T \ln N - \frac{\varepsilon^2}{2k_B T} \quad (7)$$

$$S = -\left(\frac{dA}{dT}\right) = k_B \ln N - \frac{\varepsilon^2}{2k_B T^2} \quad (8)$$

where $k_B \ln N$ is the ideal gas contribution. Hence the excess (dimensionless) entropy S_{ex} (defined by Rosenfeld), for a single particle becomes,

$$S_{\text{ex}} = \frac{S - S_{\text{id}}}{k_B} = -\frac{\varepsilon^2}{2(k_B T)^2} \quad (9)$$

from which we obtain the effective diffusion coefficient,

$$D_{\text{eff,R}} = a \exp\left(-\frac{b}{2}\beta^2 \varepsilon^2\right) \quad (10)$$

which, in essence, is equivalent to Zwanzig's expression [Eq. 3]. By comparing Eq. 3 and 10, we obtain the Rosenfeld scaling parameters as $a = D_0$, $b = 2$. The value of b is close to the values reported for this constant.

III. MODEL I. GAUSSIAN DISCRETE LATTICE

A. Description of the model

We introduce a discrete random lattice, where the energy of each site is sampled from a Gaussian distribution of mean zero and variance ε . A similar but different model of random traps and barriers was earlier introduced by Limoge and Bocquet [37], and later studied by Kehr and co-workers [38]. To contrast, the earlier model had strictly alternating barriers and traps, with a

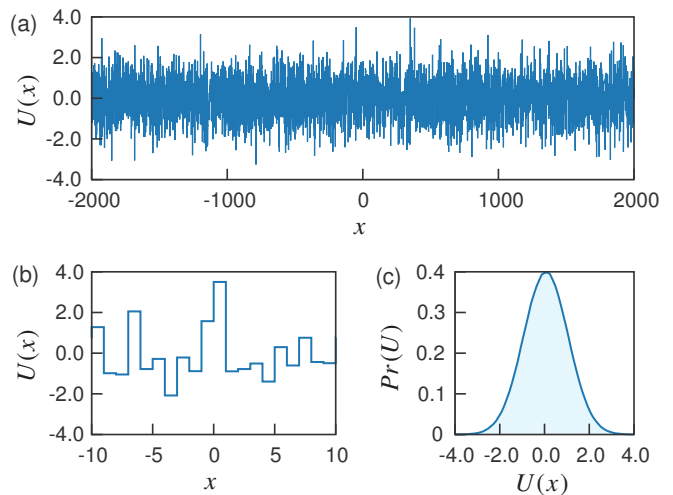


Figure 2. (a) Discrete random Gaussian potential at $\varepsilon = 1.0$. (b) Zoomed-in portion of the potential showing discrete lattice sites forming barriers and traps. (c) Distribution of the potential energy at each lattice site showing Gaussian behavior.

restriction of positive values on barrier energies and negative values on trap energies. Transitions were allowed only from one trap to the next, crossing the barrier. Our model does not restrict the energy values at individual lattice sites. Hence there can be three different scenarios,

- (i) a lower energy site neighbored by two higher energy sites (trap with barrier on both sides)
- (ii) a higher energy site neighbored by lower energy sites (barrier with trap on both sides)
- (iii) a site neighbored by higher energy on one side and lower energy on other side (barrier on one side, trap on other side)

The random walker is allowed to visit any of the neighboring sites, irrespective of the site behaving as a barrier or trap. The first case is of special interest, and we have termed it as “three-site trap (TST)” (see Fig. 1). In Fig. 2(a), we show the discrete random potential at $\varepsilon = 1.0$. The random potential consists of discrete lattice sites [see Fig. 2(b)] with the energy at each lattice site sampled from a Gaussian distribution [see Fig. 2(c)].

For particle diffusion on this potential, it seems reasonable to restrict the transitions to nearest neighbors. All transitions to neighbor sites have identical rates, if the final site has a lower energy than the initial site. Transitions that lead to energetically higher sites require thermal activation,

$$\Gamma_{i,j} = \begin{cases} \Gamma_0 & U_j < U_i \\ \Gamma_0 \exp[-\beta(U_j - U_i)] & U_j \geq U_i \end{cases} \quad (11)$$

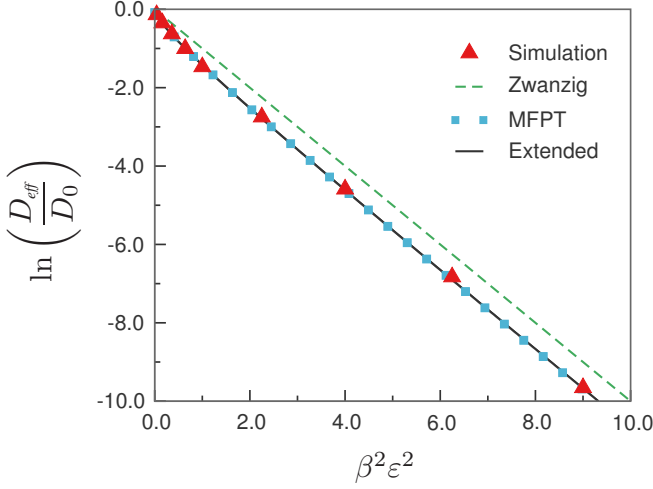


Figure 3. Semilog plot of the scaled self-diffusion coefficient D_{eff} against the squared ruggedness parameter (ε) for the discrete Gaussian random lattice. The dashed green line represents the theoretically predicted values of Zwanzig [Eq. 3]. The solid red triangles represent the results of CTRW simulation. The result obtained from numerical evaluation of MFPT [Eqs. 16 and 17] on the potential surfaces is indicated by blue squares. The solid black line shows the diffusion coefficient obtained from the corrected equation [Eq. 25].

where $\Gamma_{i,j}$ is the transition rate from site i to j and $\beta = 1/k_B T$. Transitions of this type were earlier introduced by Miller and Abrahams [39]. We perform a continuous time random walk (CTRW) on this potential, assuming $\Gamma_0 = 1$. The random walker at any site can move either to the left or to the right with rates, Γ_l and Γ_r respectively. We call a random number (r) to decide the move to the left or right with probabilities $\Gamma_l/\Gamma_{\text{tot}}$ and $\Gamma_r/\Gamma_{\text{tot}}$ where, $\Gamma_{\text{tot}} = \Gamma_l + \Gamma_r$. The time required for the move in the CTRW is given as,

$$\Delta t = -\frac{\ln r}{\Gamma_{\text{tot}}} \quad (12)$$

B. Simulation results

We perform CTRW of a Brownian particle on the discrete lattice for 1×10^7 steps. The mean-square displacement $\langle \Delta x^2 \rangle$ of the random walker gives us the effective diffusion coefficient following Einstein's relation,

$$\langle \Delta x^2 \rangle = 2D_{\text{eff}}t \quad (13)$$

where $D_{\text{eff,S}}$ denotes the D_{eff} obtained from simulation. The observed $D_{\text{eff,S}}$ with varying randomness (ε) is compared with the theoretically predicted values of Zwanzig [Eq. 3] in Fig. 3. Even at small ε , within the well-defined diffusive limit, Zwanzig's prediction is found to systematically overestimate (by a small but non-trivial amount) the simulated diffusion coefficient. *Deviation*

from Zwanzig's expression becomes large by $\varepsilon = 3.0$ where the former overestimates the simulated value by almost an order of magnitude. In contrast, the estimate of $D_{\text{eff,MFPT}}$ from the exact numerical evaluation of MFPT (see Eqs. 16 and 17 below) provides quantitative agreement with the simulation results. The corrected expression of the diffusion coefficient (see Eq. 25 below) that we have derived, also provides a quantitative agreement.

C. Numerical analysis from MFPT

To understand the deviation from Zwanzig's prediction, we looked into the validity of coarse-graining of the potential energy surface in his derivation. Without averaging over the random surface, it is possible to derive the self-diffusion coefficient using MFPT. On a segment of linear chain with $N+1$ sites, with a reflecting boundary condition at site 0 and an absorbing boundary condition at site N , an exact expression is known [40] for MFPT (τ_{MFPT}), for fixed disorder in which all transition rate for the segment appear explicitly,

$$\tau_{\text{MFPT}} = \sum_{i=0}^{N-1} \frac{1}{\Gamma_{i,i+1}} + \sum_{i=1}^{N-1} \frac{1}{\Gamma_{i,i+1}} \sum_{j=0}^{i-1} \prod_{k=j}^{i-1} \frac{\Gamma_{k+1,k}}{\Gamma_{k,k+1}} \quad (14)$$

We can consider detailed balance to be valid between two neighboring sites,

$$\rho_i \Gamma_{i,j} = \rho_j \Gamma_{j,i} \text{ with } \rho_i = \frac{\exp(-\beta U_i)}{\{\exp(-\beta U_i)\}} \quad (15)$$

where $\{\dots\}$ denote the disordered average, and the neighboring sites are given by i and j . Here, ρ_i is an occupation factor, which is proportional to the occupation probability of site i . Introducing the detailed balance condition in Eq. 14 we obtain,

$$\begin{aligned} \tau_{\text{MFPT}} &= \sum_{i=0}^{N-1} \frac{1}{\Gamma_{i,i+1}} + \sum_{i=1}^{N-1} \sum_{j=1}^i \frac{\rho_{j-1}}{\rho_i} \frac{1}{\Gamma_{i,i+1}} \\ &= \sum_{i=0}^{N-1} \frac{1}{\Gamma_{i,i+1}} + \sum_{i=1}^{N-1} \sum_{j=1}^i \frac{\exp[-\beta(U_{j-1} - U_i)]}{\Gamma_{i,i+1}} \end{aligned} \quad (16)$$

Eq. 16 gives an exact expression for the MFPT on a discrete lattice under equilibrium conditions. We calculate the MFPT on our quenched discrete potential by explicitly evaluating the summations numerically, and obtain the diffusion coefficient using the asymptotic relation,

$$D_{\text{eff,MFPT}} = \lim_{N \rightarrow \infty} \frac{N^2}{2\tau_{\text{MFPT}}} \quad (17)$$

It is to be noted here that Eq. 17 assumes that the rough energy surface can be replaced by an effective flat energy surface. As shown in Fig. 3, the numerical evaluation of $D_{\text{eff,MFPT}}$ provides quantitative agreement with

the results of CTRW on the discrete potential. We note that the MFPT explicitly takes into account the effect of TSTs, wherein a very deep trap is neighbored by two maxima. This would be neglected if one does a coarse-grained average, as in Zwanzig's treatment. Probability of occurrence of such deep traps increases with increasing randomness.

D. Theoretical derivation

With the success of numerical analysis using MFPT, one would expect a correct analytical expression for D_{eff} derived with MFPT formalism. Here we show the derivation of an elegant analytical expression for D_{eff} . We start

with Eq. 16, which on further simplification gives,

$$\tau_{MFPT} = \sum_{i=0}^{N-1} \sum_{j=0}^i \frac{\exp[-\beta(U_j - U_i)]}{\Gamma_{i,i+1}} \quad (18)$$

With no loss of generality for the system under translational invariance, we can do an averaging over the potential,

$$\tau_{MFPT} = \sum_{i=0}^{N-1} \sum_{j=0}^i \left\langle \frac{\exp[-\beta(U_j - U_i)]}{\Gamma_{i,i+1}} \right\rangle \quad (19)$$

where and below the same symbol is used for the mean first passage time and its ensemble average. By introducing the transition rate of the Miller-Abraham process, given by Eq. 11 in Eq. 19, we obtain,

$$\begin{aligned} \tau_{MFPT} &= \frac{1}{\Gamma_0} \sum_{i=0}^{N-1} \sum_{j=0}^i \left\{ \langle \exp[-\beta(U_j - U_{i+1})] \rangle_{U_{i+1} \geq U_i} + \langle \exp[-\beta(U_j - U_i)] \rangle_{U_{i+1} < U_i} \right\} \\ &= \frac{1}{\Gamma_0} \left\{ \sum_{i=0}^{N-1} \sum_{j=0}^i + \sum_{i=-1}^{N-2} \sum_{j=0}^{i-1} \right\} \langle \exp[-\beta(U_j - U_{i+1})] \rangle_{U_{i+1} \geq U_i} \end{aligned} \quad (20)$$

In the limit of $N \gg 1$ and in the absence of spatial correlation, we can simplify Eq. 20 to obtain,

$$\tau_{MFPT} = \frac{2}{\Gamma_0} \sum_{i=0}^{N-1} \sum_{j=0}^i \langle \exp(-\beta U_j) \rangle \langle \exp(\beta U_{i+1}) \rangle_{U_{i+1} \geq U_i} \quad (21)$$

The average can be taken by using the Gaussian probability distribution,

$$\langle \exp(\beta U_{i+1}) \rangle_{U_{i+1} \geq U_i} = \int_0^\infty d\Delta U_i \int_{-\infty}^\infty dU_i \exp[\beta(U_i + \Delta U_i)] P(U_i) P(U_i + \Delta U_i) \quad (22)$$

where $\Delta U_i = U_{i+1} - U_i$. Note that ΔU_i is independent of U_i in the absence of spatial correlations. The effect of spatial correlations will be studied in Sec. V. After straightforward calculation one obtains,

$$\langle \exp(\beta U_{i+1}) \rangle_{U_{i+1} \geq U_i} = \frac{1}{2} \exp\left(\frac{\beta^2 \varepsilon^2}{2}\right) \left[1 + \operatorname{erf}\left(\frac{\beta \varepsilon}{2}\right) \right] \quad (23)$$

where the right-hand side is independent of the index i owing to the translational invariance. Hence, using Eq. 23 in Eq. 21, we obtain,

$$\tau_{MFPT} = \frac{N^2}{2\Gamma_0} \exp(\beta^2 \varepsilon^2) \left[1 + \operatorname{erf}\left(\frac{\beta \varepsilon}{2}\right) \right] \quad (24)$$

In a very different context, this type of equation was obtained earlier [41]. Using Eq. 24 and 17, we get the

expression for diffusion coefficient as,

$$D_{eff} = D_0 \exp(-\beta^2 \varepsilon^2) \left[1 + \operatorname{erf}\left(\frac{\beta \varepsilon}{2}\right) \right]^{-1} \quad (25)$$

The corrected diffusion coefficient improves upon the Zwanzig's expression and quantitatively agrees with the simulation results (see Fig. 3).

IV. MODEL II. GAUSSIAN RANDOM FIELD

Our second model comprise of a continuous Gaussian random surface (or, field) $[\Phi]$ generated by random Fourier modes. Using a standard method [42], we write

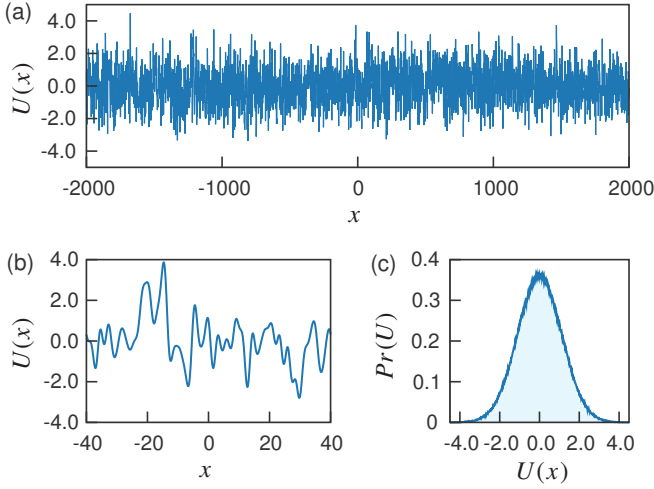


Figure 4. (a) Continuous random Gaussian field [Eq. 26] at $\varepsilon = 1.0$. (b) Zoomed-in portion of the potential showing the continuity of the surface. (c) Distribution of the potential energy showing Gaussian behavior.

the continuous random field as

$$\Phi = \varepsilon \sqrt{\frac{2}{M}} \sum_{n=1}^M \cos(\mathbf{k}_n \cdot \mathbf{x} + \theta_n) \quad (26)$$

where M is the number of modes chosen, \mathbf{k}_n is a random wave vector chosen independently from a Gaussian distribution of mean zero and variance σ (we use $\sigma = 1$), θ_n is a random phase chosen from a uniform distribution between 0 and 2π . It can be shown that Φ has a Gaussian distribution with mean zero and variance ε . In Fig. 4, we show a realization of continuous random surface at $\varepsilon = 1.0$. It has been generated using 200 random modes ($M = 200$). At smaller length scales, one can note the continuity of the potential Fig. 4(b). The distribution of the potential energy of this lattice is shown in Fig. 4(c). Study of random walks on Gaussian random fields has generated a lot of interest in recent years [29, 43–45]. The continuity of such a field helps us to perform continuous Brownian Dynamics (BD), thereby providing an opportunity to probe the detailed dynamics of the system.

We perform BD (using second-order Runge-Kutta method) on this Gaussian field with 1000 particles starting from random positions. The effective diffusion coefficient obtained from the Brownian Dynamics simulation is compared with the Zwanzig’s expression in Fig. 5. Contrary to the discrete model, the simulation results corroborates with Zwanzig’s expression. As we show below, the *surprising* agreement is because of the nature of the potential surface. The three-site traps (TSTs), which were increasingly dominant in the discrete model, become negligible due to the inherent correlation in the

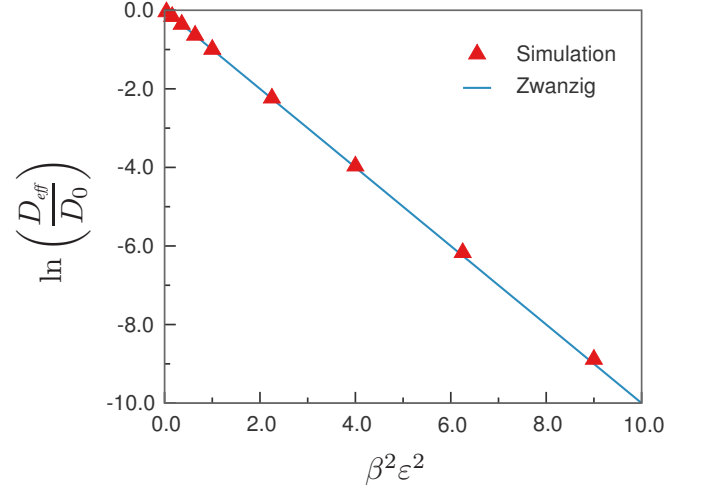


Figure 5. Semilog plot of the scaled self-diffusion coefficient D_{eff} against the squared ruggedness parameter (ε) for the continuous Gaussian random field. The solid blue line shows the theoretically predicted values of Zwanzig [Eq. 3], while the solid red triangles are the results of simulation.

continuous potential surface.

$$\langle \Phi(x) \Phi(x + \Delta x) \rangle = \varepsilon^2 \exp\left(-\frac{\sigma^2(\Delta x)^2}{2}\right) \quad (27)$$

Due to the presence of this spatial correlation, the correction term for the continuous potential becomes negligible.

V. ROLE OF SPATIAL CORRELATION

A major motivation of the present work is to investigate the role of spatial correlations in the energy landscape on the self-diffusion coefficient. Examples of such correlations are abundant in nature. For example, correlations are known [46–48] to be present in the DNA sequence that a protein experiences during search for its specific binding site. Similar correlations are also present in the landscapes of protein folding [21, 22] and glassy dynamics [23]. Here, we study the effect of correlation in the discrete lattice model (in the same spirit of the inherent correlation present in the Gaussian random field – Eq. 27), such that

$$\langle U_j U_i \rangle = \varepsilon^2 \exp\left(-\frac{\sigma^2(j-i)^2}{2}\right) \quad (28)$$

where σ is now a measure of the spatial correlation on the lattice. We derived the diffusion coefficient on this correlated potential using MFPT formalism,

$$D_{eff} = D_0 \exp(-\beta^2 \varepsilon^2) \left[1 + \operatorname{erf}\left(\frac{\beta \varepsilon}{2} \sqrt{1 - \exp\left(-\frac{\sigma^2}{2}\right)}\right) \right]^{-1} \quad (29)$$

This is a general expression of diffusion coefficient on a random lattice. On an uncorrelated surface, *i.e.* in the limit of $\sigma \rightarrow \infty$ the above expression reduces to Eq. 25.

The diffusion coefficient on the continuous potential surface can be derived using adjoint operator technique [4]. Considering a reflecting boundary condition at $x = 0$ and an absorbing boundary condition at $x = L$, the τ_{MFPT} on the continuous potential surface $U(x)$ is obtained as,

$$\tau_{\text{MFPT}} = \frac{1}{D_0} \int_0^L e^{\beta U(x)} dx \int_0^x e^{-\beta U(y)} dy \quad (30)$$

Using the same technique as used in the discrete model, the MFPT is then compared with that of a flat energy surface with same boundary conditions. Assuming that the rough energy surface can be replaced by an effective flat energy surface, the effective diffusion coefficient is subsequently obtained from,

$$D_{\text{eff}} = \lim_{L \rightarrow \infty} \frac{L^2}{2\tau_{\text{MFPT}}} \quad (31)$$

Under translation invariance, Eq. 30 can be rewritten as,

$$\tau_{\text{MFPT}} = \frac{1}{D_0} \int_0^L d\xi (L - \xi) \langle e^{\beta U(0) - \beta U(\xi)} \rangle \quad (32)$$

By substituting continuous limit of Eq. 28 into the above expression, we can calculate the MFPT using

$$\langle e^{\beta U(0) - \beta U(\xi)} \rangle = \exp(\beta^2 \langle U(0)^2 \rangle - \beta^2 \langle U(0)U(\xi) \rangle) \quad (33)$$

and obtain the effective diffusion coefficient from Eq. 31,

$$D_{\text{eff}} = \lim_{L \rightarrow \infty} \frac{D_0 L^2 \exp(-\beta^2 \varepsilon^2)}{2 \int_0^L d\xi (L - \xi) \exp\left[-\beta^2 \varepsilon^2 \exp\left(-\sigma^2 \frac{\xi^2}{2}\right)\right]} \quad (34)$$

We find that the diffusion coefficient for the correlated discrete potential – Eq. 29 and the continuous potential (which is inherently correlated) – Eq. 34 have similar implications. In the limit of $\sigma \rightarrow 0$, *i.e.* when the lattice is infinitely correlated, D_{eff} obtained from Eq. 29 reduces to Zwanzig's form, $D_{\text{eff},Z}$. Similarly, the extension term in Eq. 34 also approaches 1. Therefore, Zwanzig's expression can be regarded as a limiting form in the case of infinitely long-range correlation. This explains the reason for the agreement observed in Fig. 5.

VI. APPARENT BREAKDOWN OF ERGODICITY WITH INCREASING RUGGEDNESS

The present model provides a remarkably direct approach to study the relationship between diffusion and

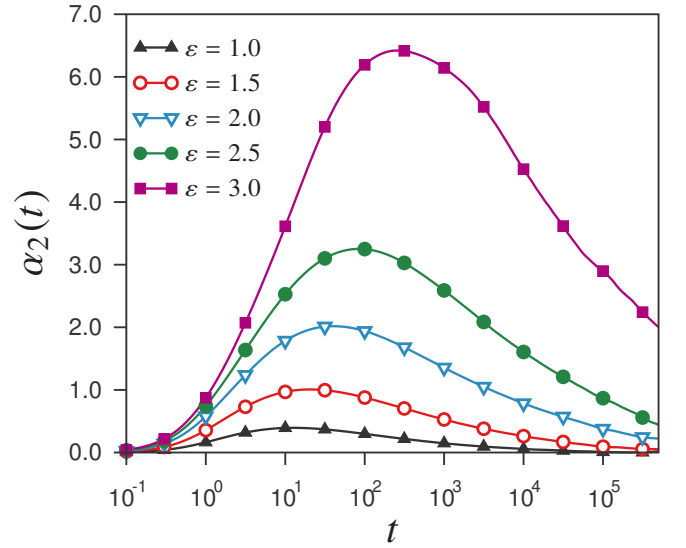


Figure 6. Non-Gaussian parameter $\alpha_2(t)$ for different randomness (ε) in the continuous Gaussian random field. The deviation from Gaussian behavior increases with increasing ε . The deviation apparent breakdown of ergodicity in the system. Hence reaching the diffusive limit becomes increasingly difficult.

ergodicity. At large ruggedness (large ε) our simulations tend to remain in the sub-diffusive regime. Even for $\varepsilon > 3.0$ we could not reach the ergodic limit. The difficulty of reaching the ergodic limit with increasing ε can be investigated using the non-Gaussian parameter, $\alpha_2(t)$. It quantifies the deviation of the distribution of displacements from a Gaussian shape and is defined as [49],

$$\alpha_2(t) = \frac{\langle \Delta x^4(t) \rangle}{\left(1 + \frac{2}{d}\right) \langle \Delta x^2(t) \rangle^2} - 1 \quad (35)$$

where d is the dimensionality of the system (in our case, $d = 1$). For an ergodic system, the mean square displacement of a particle increases linearly in time, and the van Hove self-correlation function has a Gaussian shape. In this case the non-Gaussian parameter is zero. However, a non-zero value of non-Gaussian parameter signifies a non-ergodic behavior. The evolution of $\alpha_2(t)$ with increasing ε for the continuous potential model is shown in Fig. 6. With increasing ε , the deviation from Gaussian behavior becomes more prominent. It indicates a very slow approach to diffusive behavior for higher ε that is expected to be re-established at very long times (which should scale with ε). The peak maxima τ_α gradually increases and shifts to longer time. The time τ_α depends strongly on ε and as shown in Fig. 7 can be fitted to a power law,

$$\tau_\alpha = a\varepsilon^b + c \quad (36)$$

The obtained fitting parameters are $a = 0.182, b =$

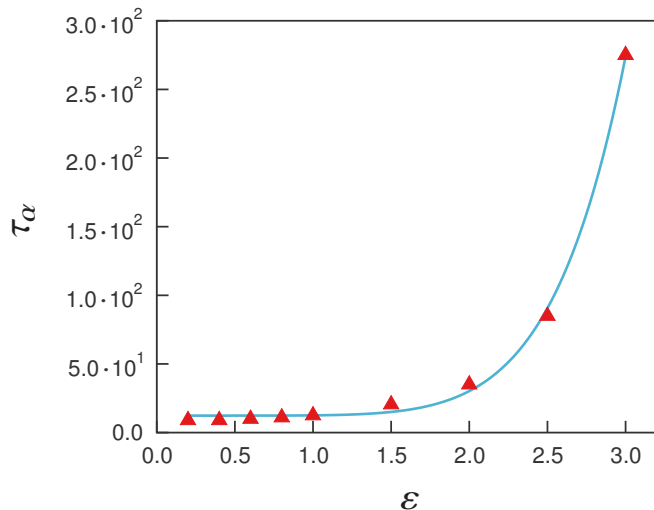


Figure 7. Dependence of peak-maxima τ_α of the non-Gaussian parameter, on the magnitude of ruggedness parameter ε of the corresponding potential energy surface. The red triangles are the results from simulations. The solid blue line is the fitting to a power law, $\tau_\alpha = 0.182\varepsilon^{6.618} + 12.363$ (see Eq. 36).

6.618 and $c = 12.363$. This clearly indicates that beyond certain ε , one needs exceedingly long time to reach the diffusive limit.

VII. CONCLUSION

The present study demonstrates that even such apparently simple models of diffusion on a random Gaussian energy surface can reproduce many of the features observed in real experimental systems, such as crossover from ergodic to non-ergodic behavior, sharp rise in the peak of the non-Gaussian parameter and sub-diffusive dynamics. On the theoretical side, there are fundamental issues that need to be overcome. The breakdown of Zwanzig's elegant expression was perhaps anticipated but

was not clearly demonstrated earlier. We introduced an extension term that rectifies Zwanzig's expression and we recommend that Eq. 25 be used instead of Zwanzig's expression for a random uncorrelated Gaussian surface. Similarly, Eq. 34 is the correct form to use for a Gaussian field. We discuss the role of spatial correlation in a random landscape, and show that Zwanzig's expression is valid in the asymptotic limit of infinitely correlated Gaussian random energy surface. The present models can be extended to treat many interesting issues [50] more quantitatively. In a future work, we shall address a dynamic derivation of Rosenfeld scaling relation.

Our discussion is restricted to one-dimensional diffusion and there seems to be no generalization to higher dimensions. While one may conjecture that this provides an insight to the multi-dimensional surface, the problem remains open for future investigation. Several interesting phenomena might appear in higher dimensions. Particularly, the walker should be able to avoid the deep minima and maxima formed by the three sites as discussed above, due to presence of alternate paths that would avoid those barriers. As a result, the mean field treatment of Zwanzig is expected to hold as dimension goes to infinity. Recent studies [28, 29] have focused on extending techniques of efficient importance sampling schemes for simulating rare events associated with higher dimensions. Such multiple scale techniques would allow further analysis on this interesting problem.

ACKNOWLEDGMENTS

We dedicate this work to Professor Robert W. Zwanzig, a pioneer and giant in the area of statistical mechanics, who served as a mentor, directly to one of us (BB) and to many others through his highly insightful papers and clear writings.

We thank Dr. R. S. Singh for many helpful discussions and critical comments. This work was supported in parts by grants from Board of Research in Nuclear Sciences (BRNS) and Department of Science and Technology (DST), India. BB acknowledges support from J. C. Bose Fellowship (DST).

-
- [1] B. Bagchi, *Molecular Relaxation in Liquids* (Oxford University Press, USA, 2012).
 - [2] S. Lifson and J. L. Jackson, *J. Chem. Phys.* **36**, 2410 (1962).
 - [3] E. W. Montroll and G. H. Weiss, *J. Math. Phys.* **6**, 167 (1965).
 - [4] G. H. Weiss, "Advances in chemical physics," (John Wiley & Sons, Inc., 2007) pp. 1–18.
 - [5] R. Zwanzig, *Proc. Natl. Acad. Sci. USA* **85**, 2029 (1988).
 - [6] H. Frauenfelder, S. G. Sligar, and P. G. Wolynes, *Science* **254**, 1598 (1991).
 - [7] F. H. Stillinger, *Science* **267**, 1935 (1995).
 - [8] C. A. Angell, *Science* **267**, 1924 (1995).
 - [9] M. D. Ediger, C. A. Angell, and S. R. Nagel, *J. Phys. Chem.* **100**, 13200 (1996).
 - [10] Y. Kafri, D. K. Lubensky, and D. R. Nelson, *Biophys. J.* **86**, 3373 (2004).
 - [11] P. C. Blainey, G. Luo, S. C. Kou, W. F. Mangel, G. L. Verdine, B. Bagchi, and X. S. Xie, *Nat. Struct. Mol. Biol.* **16**, 1224 (2009).
 - [12] J.-H. Jeon, V. Tejedor, S. Burov, E. Barkai, C. Selhuber-Unkel, K. Berg-Sørensen, L. Oddershede, and R. Metzler, *Phys. Rev. Lett.* **106**, 048103 (2011).
 - [13] I. Golding and E. C. Cox,

- Phys. Rev. Lett. **96**, 098102 (2006).
- [14] K. A. Dill, Biochemistry **24**, 1501 (1985).
 - [15] J. D. Bryngelson and P. G. Wolynes, Proc. Natl. Acad. Sci. USA **84**, 7524 (1987).
 - [16] J. D. Bryngelson and P. G. Wolynes, J. Phys. Chem. **93**, 6902 (1989).
 - [17] K. A. Dill, S. B. Ozkan, M. S. Shell, and T. R. Weikl, Annu. Rev. Biophys. **37**, 289 (2008).
 - [18] B. P. English, W. Min, A. M. van Oijen, K. T. Lee, G. Luo, H. Sun, B. J. Cherayil, S. C. Kou, and X. S. Xie, Nat. Chem. Biol. **2**, 87 (2006).
 - [19] W. Min, B. P. English, G. Luo, B. J. Cherayil, S. C. Kou, and X. S. Xie, Acc. Chem. Res. **38**, 923 (2005).
 - [20] H. Scher and M. Lax, Phys. Rev. B **7**, 4491 (1973).
 - [21] B. A. Shoemaker, J. Wang, and P. G. Wolynes, **94**, 777 (1997).
 - [22] S. S. Plotkin, J. Wang, and P. G. Wolynes, J. Chem. Phys. **106**, 2932 (1997).
 - [23] Jin Wang, Steven S. Plotkin, and Peter G. Wolynes, J. Phys. I France **7**, 395 (1997).
 - [24] R. Metzler and J. Klafter, Phys. Rep. **339**, 1 (2000).
 - [25] J. W. Haus, K. W. Kehr, and J. W. Lyklema, Phys. Rev. B **25**, 2905 (1982).
 - [26] J. Bernasconi, H. U. Beyeler, S. Strässler, and S. Alexander, Phys. Rev. Lett. **42**, 819 (1979).
 - [27] R. L. Jack and P. Sollich, J. Stat. Mech. Theor. Exp. **2009**, P11011 (2009).
 - [28] P. Dupuis, K. Spiliopoulos, and H. Wang, in *Proceedings of the 2011 Winter Simulation Conference (WSC)* (IEEE, 2011) pp. 504–515.
 - [29] P. Dupuis, K. Spiliopoulos, and H. Wang, Multiscale Model. Simul. **10**, 1 (2012).
 - [30] D. L. Stein and C. M. Newman, Phys. Rev. E **51**, 5228 (1995).
 - [31] Y. Rosenfeld, Chem. Phys. Lett. **48**, 467 (1977).
 - [32] Y. Rosenfeld, Phys. Rev. A **15**, 2545 (1977).
 - [33] M. Agarwal and C. Chakravarty, Phys. Rev. E **79**, 030202 (2009).
 - [34] T. Goel, C. N. Patra, T. Mukherjee, and C. Chakravarty, J. Chem. Phys. **129**, 164904 (2008).
 - [35] G. Adam and J. H. Gibbs, J. Chem. Phys. **43**, 139 (1965).
 - [36] P. G. Wolynes, J. Res. Natl. Inst. Stand. Technol. **102**, 187 (1997).
 - [37] Y. Limoge and J. L. Bocquet, Phys. Rev. Lett. **65**, 60 (1990).
 - [38] K. Mussawisade, T. Wichmann, and K. W. Kehr, J. Phys.: Condens. Matter **9**, 1181 (1997).
 - [39] A. Miller and E. Abrahams, Phys. Rev. **120**, 745 (1960).
 - [40] K. P. N. Murthy and K. W. Kehr, Phys. Rev. A **40**, 2082 (1989).
 - [41] H. Cordes, S. D. Baranovskii, K. Kohary, P. Thomas, S. Yamasaki, F. Hensel, and J.-H. Wendorff, Phys. Rev. B **63**, 094201 (2001).
 - [42] R. H. Kraichnan, J. Fluid Mech. **77**, 753 (1976).
 - [43] S. Olla and P. Siri, Stoch. Proc. Appl. **109**, 317 (2004).
 - [44] R. Rhodes, Probab. Theory Related Fields **143**, 545 (2009).
 - [45] R. Rhodes, Ann. Inst. Henri Poincaré Probab. Stat. **45**, 981 (2009).
 - [46] C.-K. Peng, S. V. Buldyrev, A. L. Goldberger, S. Havlin, F. Sciortino, M. Simons, and H. E. Stanley, Nature **356**, 168 (1992).
 - [47] S. V. Buldyrev, A. L. Goldberger, S. Havlin, R. N. Mantegna, M. E. Matsu, C.-K. Peng, M. Simons, and H. E. Stanley, Phys. Rev. E **51**, 5084 (1995).
 - [48] S. V. Buldyrev, in *Power Laws, Scale-Free Networks and Genome Bioinformatics* (Molecular Biology Intelligence Unit (Springer US, 2006) pp. 123–164.
 - [49] A. Rahman, Phys. Rev. **136**, A405 (1964).
 - [50] C. M. Newman and D. L. Stein, Ann. Inst. Henri Poincaré (B) Probab. Stat. **31**, 249 (1995).